RAPID COMMUNICATIONS

PHYSICAL REVIEW FLUIDS **1**, 082401(R) (2016)

Scaling properties of the mean wall-normal velocity in zero-pressure-gradient boundary layers

Tie Wei*
Department of Mechanical Engineering, New Mexico Institute of Mining and Technology, Socorro, New Mexico 87801-4797, USA

Joseph Klewicki†
Department of Mechanical Engineering, University of New Hampshire, Durham, New Hampshire 03824, USA and Department of Mechanical Engineering, University of Melbourne, Melbourne, Victoria 3010, Australia
(Received 26 August 2016; published 7 December 2016)

The scaling properties of the mean wall-normal velocity $V(x,y)$ in zero-pressure-gradient laminar and turbulent boundary-layer flows are investigated using numerical simulation data, physical experiment data, and integral analyses of the governing equations. The maximum mean wall-normal velocity V_∞ and the boundary-layer thickness δ are evidenced to be the proper scaling for V over most if not all of the boundary layer. This is different from the behavior of the mean streamwise velocity U or the turbulent shear stress $T = -\rho\langle uv\rangle$, which depend on different characteristic length scales in the regions near and away from the surface, respectively. The reason for this apparent difference in scaling behaviors is described physically relative to the downstream development of the U velocity profile and the mechanisms of boundary-layer growth. Insights pertaining to this are further surmised from an analytical relationship for the ratio of the displacement to momentum thickness, i.e., shape factor H. Integral analyses using the continuity and mean momentum equation show that $U_\infty V_\infty/u_\tau^2 = H$, where u_τ is the friction velocity. Both the laminar similarity solution and direct numerical simulation data in post-transitional flows convincingly support this relation. Over the transitional regime, data of sufficiently high quality are lacking to check if this relation remains valid.

DOI: 10.1103/PhysRevFluids.1.082401

I. INTRODUCTION

The dynamics and Reynolds number scaling behaviors of the zero-pressure-gradient (ZPG) turbulent boundary-layer (TBL) flow have received continuous attention for more than a century [1–5]. Despite the wealth of knowledge accumulated over this time frame, the fundamental understanding of how the relevant variables describing this canonical flow are interconnected remains incomplete. In particular, while the scaling properties of the mean streamwise velocity U and the turbulent shear stress $T = -\rho\langle uv\rangle$ have been well studied and documented, the properties of the mean wall-normal velocity V and its scaling behaviors have received little attention. These behaviors, however, connect to the important processes of freestream momentum entrainment and boundary-layer growth.

The lack of studies and understanding of $V(x,y)$ can be attributed to at least two inter-related reasons. One is that, owing to its small magnitude, in physical experiments V is extremely challenging (practically impossible in many cases) to accurately measure. For example, the maximum mean wall-normal velocity V_∞ is only about 0.33% of the maximum streamwise velocity U_∞ in the $\mathrm{Re}_\theta \simeq 670$ direct numerical simulation (DNS) employed herein. ($\mathrm{Re}_\theta = U_\infty\theta/\nu$, where θ is the momentum deficit thickness and ν is the kinematic viscosity.) Moreover, the ratio V_∞/U_∞ diminishes further as

*tie.wei@nmt.edu
†joe.klewicki@unh.edu; klewicki@unimelb.edu.au

the Reynolds number increases, in accord with the boundary-layer approximation. Another reason for the lack of attention to V is the notion that V, due to its small magnitude, plays an insignificant role in the structure of TBL flows. Consideration of the mean continuity equation $\partial U/\partial x + \partial V/\partial y = 0$ is, however, sufficient to appreciate the relevance of V to downstream flow development. Namely, this equation indicates that accurately predicting V is, for example, a sensitive measure of whether boundary-layer simulations accurately capture phenomena impacting boundary-layer growth.

In the remainder of this paper we first describe the scaling behaviors of the V profile in the turbulent regime. This is followed by an integral-based development revealing the relation $U_\infty^+ V_\infty^+ = H$ (or, equivalently, $V_\infty/U_\infty = 1/2C_f H$). Here a superscript $+$ denotes normalization using the kinematic viscosity ν and friction velocity $u_\tau = \sqrt{\tau_{\text{wall}}/\rho}$, where τ_{wall} is the mean wall shear stress, ρ is the fluid density, and C_f is the skin friction coefficient. The validity of this relation is analytically verified for laminar flow and is shown to hold to very good accuracy in the turbulent regime. Over the transitional regime it is difficult to test the validity of this relation owing to the lack of sufficiently high quality, and this matter is briefly discussed.

II. SCALING OF V

In the canonical turbulent boundary layer, the mean velocity components and mean stresses vary in the wall-normal direction. In general, the nature of this variation depends on the Reynolds number of the flow. Under proper normalization, profiles from different Reynolds number flows (e.g., at varying x positions) can, however, be rendered invariant over part or all of the flow. These normalizations are useful in organizing data and naturally improve understanding of flow physics. Accordingly, investigations into identifying self-similar scalings constitute a persistent focus of wall turbulence research.

The scaling properties of the mean streamwise velocity U and turbulent shear stress T have been studied extensively. Classical analyses inform us that the friction velocity is the proper velocity scale everywhere. The inner normalized mean streamwise velocity is commonly defined as $U^+ = U(x,y)/u_\tau$ and the inner normalized turbulent shear stress as $T^+ = T(x,y)/\rho u_\tau^2$. On the other hand, two characteristic lengths are traditionally employed for the profiles of U and T, inner scaling for the region close to the surface and outer scaling for the region away from the surface. The characteristic length scale in the inner region is the viscous length scale ν/u_τ and the inner normalized distance from the surface is commonly defined as $y^+ = y/(\nu/u_\tau)$. Over a region near the wall, profiles of U^+ (or T^+) from different Reynolds numbers fall onto a single curve when plotted versus y^+.

Under initial consideration, one might expect that inner scaling should also apply to the mean wall-normal velocity profile in the inner region. To explore this, Fig. 1(a) plots V^+ from different Reynolds numbers as a function of y^+. The data of Fig. 1 come from the DNS-based studies of Simens *et al.* [6] and Schlatter and Örlü [7]. Distinct from U^+ or T^+, the V^+ profiles from different Reynolds numbers do not fall on a single curve, indicating that inner normalization does not scale the data. With increasing Reynolds number, Fig. 1(a) shows that V_∞^+ becomes smaller. The dependence of V_∞^+ on the Reynolds number is clarified below.

In the outer region (away from the surface), it is generally accepted that the proper length scale is the boundary-layer thickness δ or some other integral measure of the layer thickness. For example, T^+ data from different Reynolds numbers closely follow a single curve in the region beyond the peak in T when plotted against $\eta = y/\delta$. Figure 1(b) plots V^+ against y/δ. These V^+ profiles clearly do not merge, suggesting that u_τ is not the proper velocity by which to scale the mean wall-normal velocity in the outer region.

Guided by the above observations, a number of other normalizations were investigated. Overall, these efforts uncovered that the V data appear to follow a single curve when normalized by the maximum mean wall-normal velocity V_∞ and plotted versus η. This normalization is illustrated in Fig. 2. Here it is seen that the V/V_∞ profiles from different Reynolds numbers convincingly follow a single curve when plotted versus y/δ. To better show the behavior of this normalization in the inner region, Fig. 2(b) replots the same data on log-linear axes. By noting that the onset

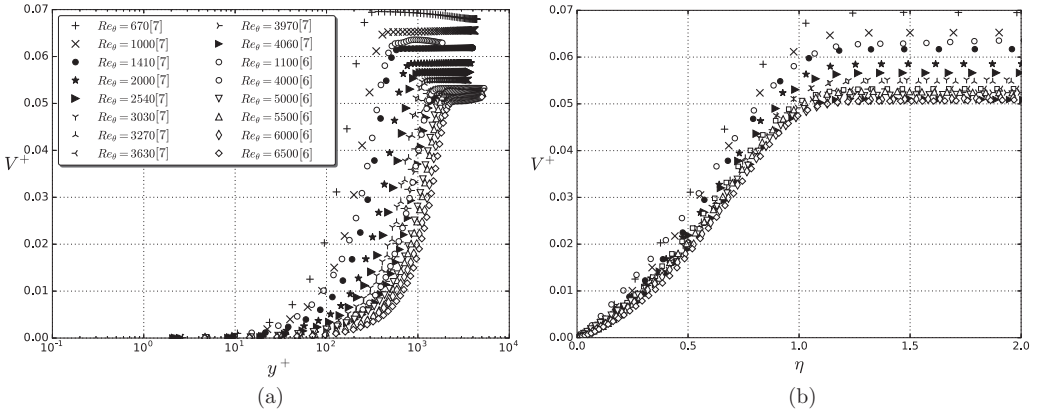

(a) (b)

FIG. 1. Scaling of the mean wall-normal flow. (a) Inner normalized V^+ versus y^+ on log-linear axes to better show the near surface region. (b) Inner normalized V^+ versus outer normalized distance from the surface $\eta = y/\delta$. The DNS data are from Refs. [6,7].

of the asymptotic four-layer regime associated with the ordering of terms in the mean momentum balance [8] is established in the boundary layer for $\mathrm{Re}_\theta \gtrsim 900$ [9], the data of Figs. 2(a) and 2(b) evidence that the V/V_∞ versus y/δ normalization is operative over the entire boundary layer, with the small deviations coming from profiles at or near the four-layer onset. In this regard, it is relevant to specifically note that *deficit* profiles in the form of $[V_\infty - V(y)]/u_\tau$ and $[V_\infty - V(y)]/V_\infty$ reveal that the former clearly fails to scale the data, while the latter is effectively an alternate way of representing the normalization of Fig. 2.

III. INTEGRAL ANALYSIS OF ZERO-PRESSURE-GRADIENT BOUNDARY-LAYER FLOWS

Physical insights into the above scaling behaviors are gained via analysis of the momentum and continuity equations. This leads to the above-noted relation $U_\infty^+ V_\infty^+ = H$. The analysis now presented is shown for the turbulent flow case. Owing, however, to the integral properties associated with the turbulent shear stress gradient profile, this same relation is also recognized to hold for the laminar flat plate flow.

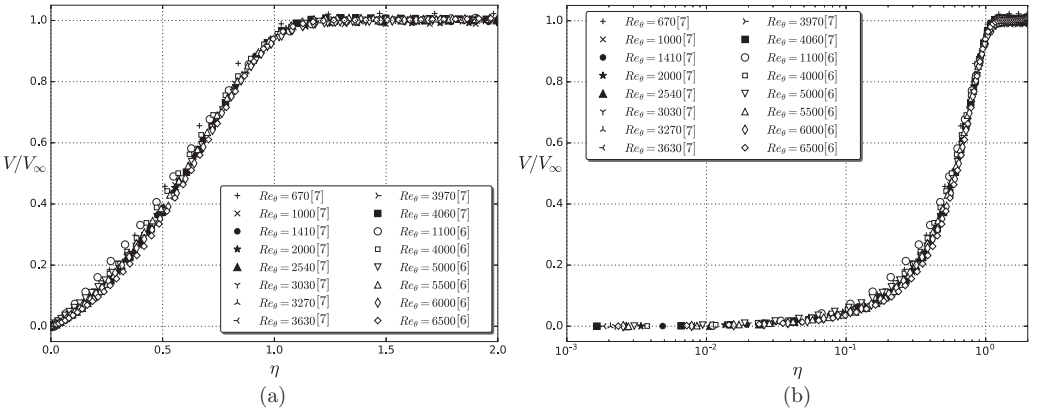

(a) (b)

FIG. 2. Plot of V/V_∞ versus $\eta = y/\delta$ on (a) linear-linear axes and (b) log-linear axes.

Under the boundary-layer approximations the continuity and streamwise mean momentum equations for the canonical ZPG TBL are

$$\frac{\partial U}{\partial x}+\frac{\partial V}{\partial y}=0, \tag{1}$$

$$U\frac{\partial U}{\partial x}+V\frac{\partial U}{\partial y}-\nu\frac{\partial^2 U}{\partial y^2}-\frac{1}{\rho}\frac{\partial T}{\partial y}=0. \tag{2}$$

Note here that the appropriate equation for laminar flow is recovered by setting $\partial T/\partial y=0$. Defining the normalized variables as

$$U^*\equiv\frac{U}{U_\infty},\quad V^*\equiv\frac{V}{U_\infty},\quad T^*\equiv\frac{T}{\rho U_\infty^2},\quad \eta\equiv\frac{y}{\delta}, \tag{3}$$

the normalized continuity and momentum equations respectively become

$$\frac{d\delta}{dx}\eta\frac{\partial U^*}{\partial\eta}-\frac{\partial V^*}{\partial\eta}=0, \tag{4}$$

$$-U^*\frac{\partial V^*}{\partial\eta}+V^*\frac{\partial U^*}{\partial\eta}-\frac{\nu}{\delta U_\infty}\frac{\partial^2 U^*}{\partial\eta^2}-\frac{\partial T^*}{\partial\eta}=0. \tag{5}$$

Integrating these equations from $\eta=0$ to $\eta=1$ yields

$$\frac{U_\infty}{V_\infty}\frac{d\delta}{dx}=\frac{1}{1-\int_0^1 U^* d\eta}, \tag{6}$$

$$-\frac{d\delta}{dx}\left(1-\int_0^1 U^{*2}d\eta\right)+\frac{V_\infty}{U_\infty}+\frac{u_\tau^2}{U_\infty^2}=0, \tag{7}$$

where the appearance of the friction velocity follows from its relation to the wall shear stress. The definition of displacement thickness δ_1 is

$$\delta_1\equiv\int_0^\infty(1-U^*)dy\approx\delta\int_0^1(1-U^*)d\eta=\delta\left(1-\int_0^1 U^*d\eta\right) \tag{8}$$

and the definition of momentum thickness θ is

$$\theta\equiv\int_0^\infty U^*(1-U^*)dy\approx\delta\int_0^1 U^*(1-U^*)d\eta=-\delta\left(1-\int_0^1 U^*d\eta\right)+\delta\left(1-\int_0^1 U^{*2}d\eta\right). \tag{9}$$

Thus the shape factor H becomes

$$H\equiv\frac{\delta_1}{\theta}=\frac{1}{\frac{1-\int_0^1 U^{*2}d\eta}{1-\int_0^1 U^*d\eta}-1}. \tag{10}$$

Combining Eqs. (6), (7), and (10) then yields

$$U_\infty^+V_\infty^+=H. \tag{11}$$

Provided the boundary-layer approximation holds, Eq. (11) is valid for any ZPG boundary layer, including laminar, transitional, and turbulent flows. We now employ further analysis and data comparisons to examine the veracity of Eq. (11).

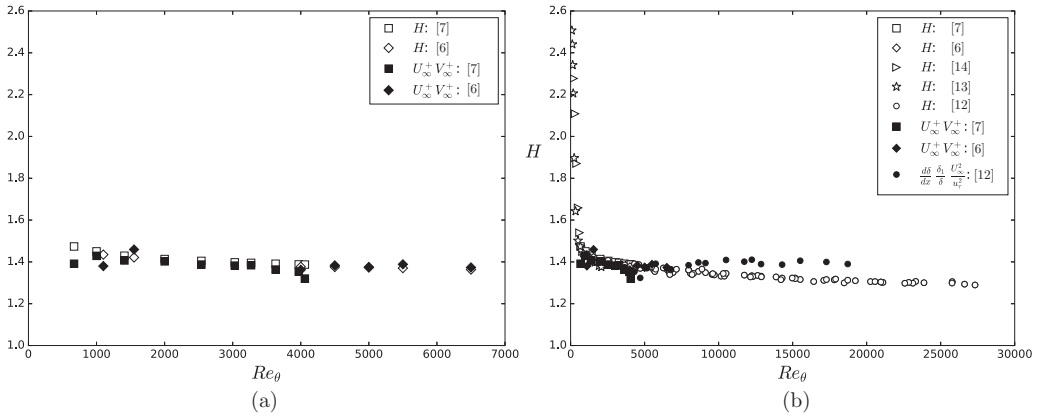

FIG. 3. Comparison of $U_\infty^+ V_\infty^+$ and H with (a) DNS data of [6,7] and (b) experimental [12,13] and other DNS data [14].

IV. TESTING $U_\infty^+ V_\infty^+ = H$

A. Laminar flow

For the case of the laminar flat plate boundary layer, we turn to the well-known results derived from the similarity solution of the Blasius [10]. Here the relationships for the displacement and momentum thicknesses are respectively given by

$$\frac{\delta_1}{x} = \frac{1.72}{\sqrt{U_\infty x/\nu}}, \quad \frac{\theta}{x} = \frac{0.664}{\sqrt{U_\infty x/\nu}} \tag{12}$$

and thus $H \simeq 2.59$. Similarly, the relationships for the skin friction and the ratio of freestream velocity components are respectively given by

$$C_f = \frac{2}{U_\infty^{+2}} = \frac{0.664}{\sqrt{U_\infty x/\nu}}, \quad \frac{V_\infty}{U_\infty} = \frac{V_\infty^+}{U_\infty^+} = \frac{0.8604}{\sqrt{U_\infty x/\nu}}. \tag{13}$$

Combining these relations yields

$$U_\infty^+ V_\infty^+ \simeq 2.59 = H. \tag{14}$$

This provides an analytical verification of the relation $U_\infty^+ V_\infty^+ = H$ for the laminar case.

B. Turbulent flow

Data for H and $U_\infty^+ V_\infty^+$ in transitional and turbulent flows are accessible from numerical simulations and reasonably from some physical experiments. This section examines data from the low-Reynolds-number turbulent regime. Through the transitional regime, the balance of terms across the boundary layer undergoes a complex evolution with Reynolds number, but eventually settles into an organized structure in which the leading terms are well defined on four distinct layers [8]. This structure is obtained at $\mathrm{Re}_\theta \simeq 900$ ($\delta^+ \simeq 370$), and for all higher Reynolds numbers the leading balances defining each layer follow well-characterized scaling behaviors and become increasingly exact as $\mathrm{Re}_\theta \to \infty$ [11]. Figure 3(a) compares DNS data of $U_\infty^+ V_\infty^+$ and H in the turbulent regime. Overall the agreement is seen to be good, with the data scatter likely due to the numerical uncertainty in the prediction of V_∞^+. Unfortunately, the Reynolds-number range of DNS data is rather limited, while high-quality direct experimental measurements of V are very scarce (virtually nonexistent).

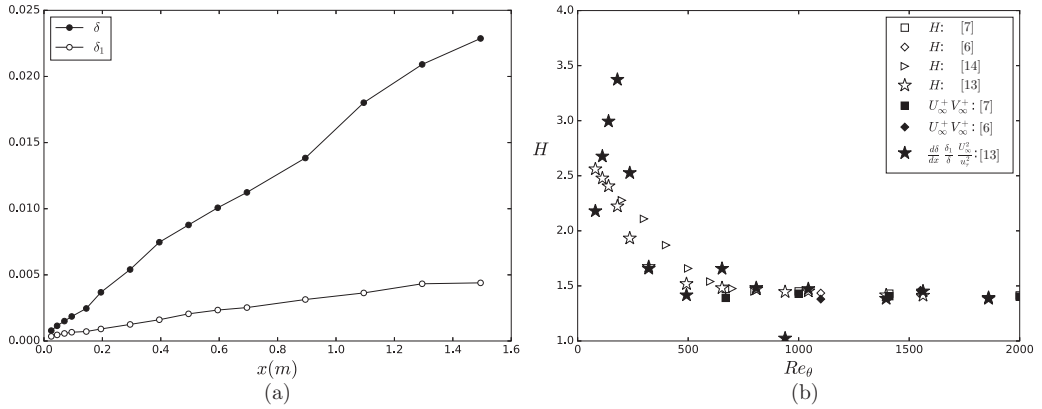

FIG. 4. (a) Streamwise growth of boundary-layer thickness δ and displacement thickness δ_1. (b) Comparison of $U_\infty^+ V_\infty^+$ and H in the transitional regime.

If, however, experimental data are available to extract the boundary-layer thickness growth rate $d\delta/dx$, Eq. (15) can be used to estimate $U_\infty^+ V_\infty^+$:

$$\frac{U_\infty}{V_\infty}\frac{d\delta}{dx} = \frac{\delta}{\delta_1} \Rightarrow U_\infty^+ V_\infty^+ = \frac{d\delta}{dx}\frac{\delta_1}{\delta}\frac{2}{C_f}. \tag{15}$$

In many experimental studies of boundary-layer flows, measurements of δ, δ_1, and C_f are provided. If the mean streamwise velocity profiles are measured at a few streamwise stations under the same flow conditions, then $d\delta/dx$ can be estimated, giving $U_\infty^+ V_\infty^+$ from Eq. (15). Österlund [12] measured mean velocity profiles at five x stations $x = 1.5$, 2.5, 3.5, 4.5, and 5.5 m under nominally fixed U_∞ conditions. Note that the resolution in the streamwise direction is rather coarse. The results from their data at stations $x = 2.5$ and 3.5 m are presented in Fig. 3(b). These data reasonably support equality between $U_\infty^+ V_\infty^+$ and H, with the deviation most likely caused by scatter in the approximation of $d\delta/dx$, which becomes more pronounced at the first and last stations.

C. Transitional flow

Detailed experimental studies over the transitional regime are rare. One of the most comprehensive studies is the T3 bench test cases of ERCOFTAC SIG10 (T3A and T3B) [13,15]. Data from T3B case are used in Fig. 4(b) to calculate $U_\infty^+ V_\infty^+$ using Eq. (15). The difference is again likely to be attributable to the error in estimating $d\delta/dx$. For example, the large deviation in the T3B-based estimate at $\mathrm{Re}_\theta \simeq 900$ corresponds to the subtle bump in the δ profile at $x \simeq 0.9$ m in Fig. 4(a). At lower Reynolds number, the boundary layer is relatively thin and the error in estimating $d\delta/dx$ is also more pronounced. These data indicate that over the transitional regime the estimated $U_\infty^+ V_\infty^+$ has a magnitude very similar to H and nominally follows the trend over the transitional regime. Higher-quality data are, however, needed to check the validity of this relation more directly.

Direct numerical simulation is designed to capture the full physics embodied in the Navier-Stokes equations and this provides good reason to expect it to provide the most reliable data for V. Accordingly, DNS should be most appropriate for evaluating whether $U_\infty^+ V_\infty^+ = H$. In this regard, we examined a number of V profiles from transitional regime DNS [14,16,17]. All of these studies, however, produced questionable behaviors in the V profile that caused us to question whether the accuracy of transitional regime DNS is, as of yet, sufficient to test the veracity of $U_\infty^+ V_\infty^+ = H$. On the other hand, one might also expect the boundary-layer approximation to break down during at least some part of the transitional regime, as streamwise gradients in turbulence related terms are likely to be quite large. Thus, the validity of $U_\infty^+ V_\infty^+ = H$ in the transitional regime awaits further

investigation. These phenomena also further emphasize the sensitivities of early boundary-layer growth and entrainment to the inflow wall boundary condition (see, e.g., [7,18–20]).

V. SUMMARY

The present analyses indicate that the maximum mean wall-normal velocity V_∞ and the boundary-layer thickness δ are the proper parameters for scaling the mean wall-normal profile in the ZPG TBL. This single scaling appears valid over the entire boundary layer and thus is qualitatively distinct from the apparent two length scaling behaviors of U and T. Based upon the continuity equation relating the streamwise rate of change of U to the wall-normal variation of V, this outer scaling behavior is seen to connect to the streamwise increasing deficit of U momentum relative to U_∞. This interpretation is reinforced by integral analysis of the continuity and streamwise momentum equations, revealing that the product of $U_\infty^+ V_\infty^+$ equals the shape factor H. The DNS data of $U_\infty^+ V_\infty^+$ were compared with H data and the present observations in the turbulent regime support their equality.

ACKNOWLEDGMENTS

Dr. Coupland, Dr. Jimenez, Dr. Österlund, Dr. Schlatter, and Dr. Wu are gratefully acknowledged for the generous sharing of their numerical or experimental data on the web. T.W. acknowledges the support of New Mexico Institute of Mining and Technology (start-up funds). J.C.K. acknowledges the support of the National Science Foundation (Grant No. CBET-1545564) and the Australian Research Council (Grant No. DP150102593).

[1] H. Schlichting and K. Gersten, *Boundary-Layer Theory* (Springer Science & Business Media, New York, 2000).

[2] M. Gad-el Hak and P. R. Bandyopadhyay, Reynolds number effects in wall-bounded turbulent flows, Appl. Mech. Rev. **47**, 307 (1994).

[3] A. J. Smits, B. J. McKeon, and I. Marusic, High-Reynolds number wall turbulence, Annu. Rev. Fluid Mech. **43**, 353 (2011).

[4] I. Marusic, B. J. McKeon, P. A. Monkewitz, H. M. Nagib, A. J. Smits, and K. R. Sreenivasan, Wall-bounded turbulent flows at high Reynolds numbers: Recent advances and key issues, Phys. Fluids **22**, 065103 (2010).

[5] J. C. Klewicki, Reynolds number dependence, scaling, and dynamics of turbulent boundary layers, J. Fluids Eng. **132**, 094001 (2010).

[6] M. P. Simens, J. Jimenez, S. Hoyas, and Y. Mizuno, A high-resolution code for turbulent boundary layers, J. Comput. Phys. **228**, 4218 (2009).

[7] P. Schlatter and R. Örlü, Assessment of direct numerical simulation data of turbulent boundary layers, J. Fluid Mech. **659**, 116 (2010).

[8] T. Wei, P. Fife, J. C. Klewicki, and P. A. McMurtry, Properties of the mean momentum balance in turbulent boundary layer, pipe and channel flows, J. Fluid Mech. **522**, 303 (2005).

[9] J. C. Klewicki, R. Ebner, and X. Wu, Mean dynamics of transitional boundary-layer flow, J. Fluid Mech. **682**, 617 (2011).

[10] H. Blasius, Grenzschichten in Flussigkeiten mit Kleiner Reibung, Z. Math. Phys. **56**, 1 (1908).

[11] J. C. Klewicki, A description of turbulent wall-flow vorticity consistent with mean dynamics, J. Fluid Mech. **737**, 176 (2013).

[12] J. M. Österlund, Experimental studies of zero pressure-gradient turbulent boundary layer flow, Ph.D. thesis, Royal Institute of Technology, 1999.

[13] J. Coupland, ERCOFTAC special interest group on laminar to turbulent transition and retransition T3A and T3B test cases, ERCOFTAC report, 1990 (unpublished).

[14] X. Wu and P. Moin, Transitional and turbulent boundary layer with heat transfer, Phys. Fluids **22**, 085105 (2010).

[15] P. E. Roach and D. H. Brierley, in *Numerical Simulation of Unsteady Flows and Transition to Turbulence*, edited by O. Pironneau, W. Rodi, I. L. Ryhming, A. M. Savill, and T. V. Truong (Cambridge University Press, Cambridge, 1992), p. 319.

[16] X. Wu and P. Moin, Direct numerical simulation of turbulence in a nominally zero-pressure-gradient flat-plate boundary layer, J. Fluid Mech. **630**, 5 (2009).

[17] T. Sayadi, C. W. Hamman, and P. Moin, Direct numerical simulation of complete H-type and K-type transitions with implications for the dynamics of turbulent boundary layers, J. Fluid Mech. **724**, 480 (2013).

[18] K. A. Chauhan, P. A. Monkewitz, and H. M. Nagib, Criteria for assessing experiments in zero pressure gradient boundary layers, Fluid Dyn. Res. **41**, 021404 (2009).

[19] N. Hutchins, Caution: Tripping hazards.J. Fluid Mech. **710**, 1 (2012).

[20] I. Marusic, K. A. Chauhan, V. Kulandaivelu, and N. Hutchins, Evolution of zero-pressure-gradient boundary layers from different tripping conditions, J. Fluid Mech. **783**, 379 (2015).